



Synthesis, Antibacterial Activity and DFT Calculations of Some Thiazolidine-4-Carboxylic acid Derivatives and Their Complexes with Cu(II), Fe(II) and VO(II)



CrossMark

Firas Abass Nawar¹, Rafid Humaidan AL-Asadi^{2*} and Dawood Salim Abid²

¹Education Directorate of Thi-Qar, Ministry of Education, Thi-Qar, Iraq.

²Department of Chemistry, College of Education for Pure Sciences, University of Basrah, Iraq.

THE reaction of L-Cysteine with 2-hydroxy naphthaldehyde and 2-hydroxy benzaldehyde yields novel bidentate ligands (2*R*,4*R*)-2-(2-hydroxynaphthalen-1-yl) thiazolidine-4-carboxylic acid (**L**²) and (2*R*,4*R*)-2-(2-hydroxyphenyl) thiazolidine-4-carboxylic acid (**L**¹), respectively, which can be characterised based on spectral and physical data. Synthesis of complexes with the formula ML₂.XH₂O is done via the reaction of **L**¹ and **L**² with Cu(II), Fe(II) and VO(II) in molar ratio of 1:2 pertaining to metal to ligand. Based on mass and UV/visible spectra, IR, flame atomic absorption, magnetic susceptibility as well as thermal analysis of metal complexes, we can conclude that the ligands behave as a bidentate and help to identify proper structure pertaining to complexes. Then, screening of the synthesized compounds is carried out to determine their antibacterial activity against *Pseudomonas aeruginosa* and *Streptococcus epidermis*. All compounds showed bio- activity with iron complexes possessing the highest efficiency. The density functional theory at the B3LYP level of theory was employed to calculate the geometry optimisation pertaining to molecular structure as well as energies of ligands and its associated complexes. The observations of the theoretical calculations were in line with the outcomes of the experiment.

Keywords: Thiazolidine-4-carboxylic acid, Antibacterial, Metal complexes, Computational study.

Introduction

Thiazolidine-4-carboxylic acid (THC), also known as thioproline, can be defined as cyclic sulphur containing amino acid, and can be easily synthesized by the reaction of L-cysteine with aromatic or aliphatic aldehydes [1-4]. This reaction yielded (2*S*,4*R*)- and (2*R*,4*R*)-diastereomer mixture. In 1936, Schubert described and synthesized thioproline and in 1937, it was done independently by Clark and Ratner [5].

In the pharmaceutical industry, thiazolidines and their derivatives find applications as potent enzyme[6], receptor antagonists and important building blocks for medicines[7,8]. Therefore,

thiazolidine-4-carboxylic acid allows restoring “contact inhibition” pertaining to tumour cells and its interaction with metal ions is regarded to be of key significance [9,10]. The derivatives pertaining to 2- substituted thiazolidine - 4- carboxylic acids find application as key intermediates in peptide synthesis [11], as well as preparation of antiviral [2], microencapsulated liposomal and immunostimulating biological drugs[7,12].

Metal complex compounds have been extensively illustrated in contemporary medicine for the diagnosis as well as treatment of human tumours. The literature contains studies on metalopharmaceutical agents being employed in the treatment of manic depression, cancer,

*Corresponding author e-mail: dr.rafid74@yahoo.com

Received 23/8/2019; Accepted 27/11/2019

DOI: 10.21608/ejchem.2019.16096.1986

© 2020 National Information and Documentation Center (NIDOC)

arthritis, as well as their application as antistatic and antimicrobial agents, and others [13,14]. This research paper describes the synthesis pertaining to certain derivatives of thiazolidine-4-carboxylic acid as well as their formation of complexes with Fe(II), Cu(II) and VO(II). Also, it includes characterisation of the synthesis compounds through different spectral techniques, assessment of antibacterial activity and then study using the DFT calculation.

Experimental

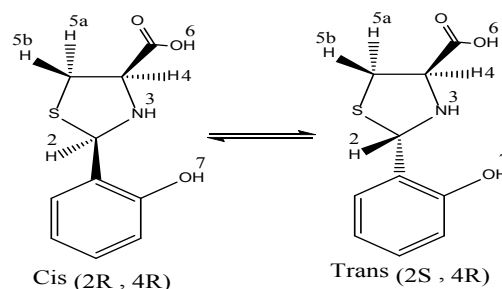
All chemicals were obtained from well-known companies such as SIGMA ALDRICH, ALDRICH, CDH and SCHARLAU and used without purification. Melting points of compounds were determined by a Thermo Scientific (9100), Electro Thermal Engineering TD, UK. Infrared spectra were recorded as KBr discs using a FT-IR spectrophotometer Shimadzu model IR.Affinity-1. UV-Visible spectra measured by Shimadzu UV-1800 using DMF as a solvent. ¹H NMR spectra of ligands were obtained on Bruker 400 MHz spectrometer using DMSO-*d*₆ as a solvent and the tetramethyl silane (TMS) as an internal reference. Mass spectra were recorded by EI Technique using Agilent Technologies spectrometers using 70 eV. Thermo gravimetric Analysis of metal complexes recorded by TGA Q50 V6.7 with heating rate 10 °C/min and in a thermal range 20-750 °C. Flame atomic absorption of metal complexes measured by Phoenix-986 Spectrometer. The magnetic susceptibility for metal complexes measured by Auto Magnetic Susceptibility Balance Sherwood. Molar electrical conductivity of metal complexes measured by Wiss-techn.Werkstätten. D 812 Weillhaim and used DMF as a solvent.

Synthesis of Ligands

(2R,4R)-2-(2-hydroxyphenyl)thiazolidine-4-carboxylic acid L¹

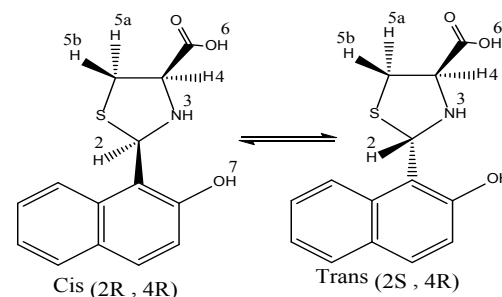
At room temperature (25-30°C), stirring was done to a mixture containing 2-hydroxy benzaldehyde (26 mmol, 3.17 g) and L-Cysteine (26 mmol, 3.15 g) in 60 mL of water and ethanol (1:1) for 24 hours. After this reaction, TLC follows the reaction completion. The precipitate was gathered through filtration and washed with diethyl ether. To obtain a white solid crystal, the solid product from a mixture of water and hot ethanol was recrystallized two times. Yield: 92%. m.p.: 158-160°C. UV-Vis. (C₂H₅OH, nm): 210 (n-σ*), 254(π-π*), 283(n-π*), 325 (π-π*). FT-IR (KBr, ν, cm⁻¹): 3450 (OH), 3101 (arom. CH), 2954 and 2900 (aliph. CH), 2694 and 2574

(Zwitter ion) 1640 (C=O), 1618 (C=C). ¹H NMR (DMSO-*d*₆, δ, ppm): *cis*-isomer (47%): 2.08 (s, 1H, H3); 2.96 (d, 1H, H5a); 3.03 (d, 1H, *J* = 5.3, H5b); 3.83 (dd, 1H, *J* = 9.1 and 6.9, H4); 5.6 (s, 1H, H2); 7.06-7.34 (m, 4H, Ar-H); 9.8 (s, 1H, H7); *trans*-isomer (53%): 2.08 (s, 1H, H3); 2.96 (d, 1H, H5a); 3.03 (d, 1H, *J* = 5.3, H5b); 4.25 (dd, 1H, *J* = 9.1 and 6.9, H4); 5.6 (s, 1H, H2); 7.06-7.34 (m, 4H, Ar-H); 9.8 (s, 1H, H7); 9.8 (s, 1H, H7). MS(EI, *m/z* (%)): 225[M⁺, 50.5].



(2R,4R)-2-(2-hydroxynaphthalen-1-yl)thiazolidine-4-carboxylic acid L²

The same procedure of L¹ was used to synthesise the ligand but employed 2-hydroxy naphthaldehyde (26 mmol, 4.47 g). This led to formation of a white yellow solid crystal. Yield: 83%. m.p.: 149-150°C. UV-Vis. (C₂H₅OH, nm): 215 (n-σ*), 281(π-π*), 293(n-π*), 318 (π-π*). FT-IR (KBr, ν, cm⁻¹): 3350 (OH), 3001 (arom. CH), 2995 (aliph. CH), 2652 (Zwitter ion) 1635 (C=O), 1587 (C=C). ¹H NMR (DMSO-*d*₆, δ, ppm): *cis*-isomer (39%): 2.03 (s, 1H, H3); 3.13 (dd, 1H, *J* = 9.3, H5a); 3.27 (dd, 1H, *J* = 10.6, H5b); 3.44 (m, 1H, H4); 6.7 (s, 1H, H2); 7.05-7.9 (m, 6H, Ar-H); 9.19 (s, 1H, H7); *trans*-isomer (61%): 2.03 (s, 1H, H3); 3.13 (dd, 1H, *J* = 9.3, H5a); 3.27 (dd, 1H, *J* = 10.6, H5b); 3.44 (m, 1H, H4); 6.51 (s, 1H, H2); 7.05-7.9 (m, 6H, Ar-H); 9.19 (s, 1H, H7). MS(EI, *m/z* (%)): 275[M⁺, 16.7].



Synthesis of complexes

Metal was added to the ligands in a 1:2 mole ratio to prepare all the complexes. 6 mmol of

metal salts were mixed with the hot methanolic solution of 15 mL, while 12 mmol of respective ligands with hot methanolic solution of 30 mL. For 6-8 hours, refluxing of the reaction mixture was done. The precipitated products were then filtered, followed by washing with water, ethanol and diethyl ether, and then subsequent drying with CaCl_2 .

[Cu(L¹)₂].H₂O: (Wt. g): L¹=2.70, CuSO₄.5H₂O=1.49. Yield: 52%. m.p.: >300°C. Color: dark brown. Uv-Vis. (C₂H₅OH, nm): 230(π - π*), 250 (π - π*), 270(C-T), 300(n - π*), 670(d-d). FTIR (KBr, ν, cm⁻¹): 3439 (OH), 3024(arom.CH), 1735 (C=O), 1622(C=C). μ_{eff}(B.M): 1.34. Molar conductivity (DMF, Ohm⁻¹ cm²mol⁻¹): 13. MS(EI, m/z (%)): 529[M⁺, 10.5].

[Fe(L¹)₂(H₂O)₂]: (Wt. g): L¹=2.70, FeSO₄.7H₂O =1.66. Yield: 77%. m.p.: >300°C. Color: light brown. Uv-Vis. (C₂H₅OH, nm): 220(π - π*), 300 (n - π*), 360(π - π*), 500(C-T), 600(d-d). FTIR (KBr, ν, cm⁻¹): 3387 (OH), 3282(arom.CH), 1672 (C=O), 1608 (C=C). μ_{eff}(B.M): 6.31. Molar conductivity (DMF, Ohm⁻¹ cm²mol⁻¹): 16. MS(EI, m/z (%)): 538[M⁺, 15].

[VO(L¹)₂].2H₂O: (Wt. g): L¹=2.70, VOSO₄.H₂O=1.08. Yield: 66%. m.p.: >300°C. Color: dark brown. Uv-Vis. (C₂H₅OH, nm): 310(π - π*), 340 (π - π*), 360(n - π*), 390(C-T), 570, 620(d-d). FTIR (KBr, ν, cm⁻¹): 3406 (OH), 3059(arom. CH), 1747 (C=O), 1635 (C=C). μ_{eff}(B.M): 1.59. Molar conductivity (DMF, Ohm⁻¹ cm²mol⁻¹): 36. MS(EI, m/z (%)): 549[M⁺, 5.5].

[Cu(L²)₂].1/2H₂O: (Wt. g): L²=3.30, CuSO₄.5H₂O=1.49. Yield: 63%. m.p.: >300°C. Color: Brown. Uv-Vis. (C₂H₅OH, nm): 230(π - π*), 260 (π - π*), 330(C-T), 660(d-d). FTIR (KBr, ν, cm⁻¹): 3475 (OH), 3111 and 3018(arom. CH), 2900 and 2825(aliph. CH), 1649 (C=O), 1622 (C=C). μ_{eff}(B.M): 1.37. Molar conductivity (DMF, Ohm⁻¹ cm²mol⁻¹): 14. MS(EI, m/z (%)): 621[M⁺, 12].

[Fe(L²)₂(H₂O)₂]: (Wt. g): L²=3.9, FeSO₄.7H₂O =1.66. Yield: 85%. m.p.: >300°C. Color: Brown. Uv-Vis. (C₂H₅OH, nm): 240(π - π*), 280 (π - π*), 310(n - π*), 380(C-T), 580 (d-d). FTIR (KBr, ν, cm⁻¹): 3313 (OH), 3062(arom.CH), 1650 (C=O), 1608 (C=C). μ_{eff}(B.M): 5.96. Molar conductivity (DMF, Ohm⁻¹ cm²mol⁻¹): 6. MS(EI, m/z (%)): 640[M⁺, 8].

[VO(L²)₂].4H₂O: (Wt. g): L²=3.9, VOSO₄.H₂O =1.08. Yield: 63%. m.p.: >300°C. Color: Black. Uv-Vis. (C₂H₅OH, nm): 220(π - π*), 290 (π - π*), 300(n - π*), 430(C-T), 570, 630(d-d). FTIR (KBr, ν, cm⁻¹): 3441 (OH), 3149(arom. CH), 1680 (C=O), 1622 (C=C). μ_{eff}(B.M): 1.68. Molar conductivity (DMF, Ohm⁻¹ cm²mol⁻¹): 33.

Antimicrobial activity

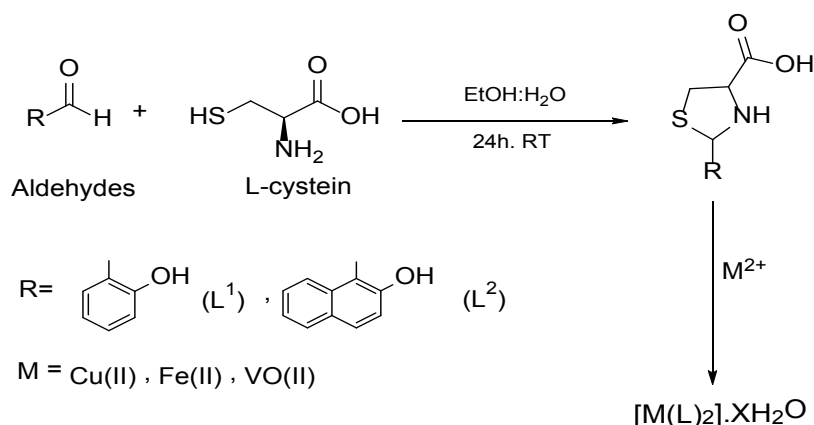
The diffusion assay agar technique [15] was deployed for gauging the bacterium's biological activity by utilising two kinds of bacteria, namely *Pseudomonas aeruginosa* and *Streptococcus epidermis*. These were added to the dishes and allowed to dry for 15 to 20 min. On the plant medium, 0.2 mm of the activated bacteria were inserted and then, with the help of perforated perforation with a diameter of 0.9 mm, the centre hole was mined. The compounds were synthesized with 1000 ppm in DMSO, wherein 0.1 mL of solution is added to dishes and then incubation is carried out for 24 hours at a temperature of 37°C. Then, a comparison of the effectiveness pertaining to inhibition of compounds is done with two standard antibiotics (Ciprofloxacin and Amoxicillin) by considering the same concentration.

Computational study

The density functional theory (DFT) method was employed to calculate the geometry optimisation as well as energies pertaining to the synthesis of compounds, at a B3LYP level of theory by considering 6-311G++(d,p) as a basis set for L² and L¹ [16], while mixed basis set 6-311++G(d,p) and LanL2DZ were employed for metal complexes molecules [17]. The Gaussian09 program was employed for calculations in gaseous phase.

Results and Discussion

This research study explains the synthesis pertaining to certain Thiazolidine-4-carboxylic acid derivatives L² and L¹, which were synthesized in good yield via the reaction of L-Cysteine with 2-hydroxy naphthaldehyde and 2-hydroxy benzaldehyde. As presented in Scheme 1, synthesis of metal complexes was achieved by the reaction of L¹ and L² with Cu(II), VO(II) and Fe(II) ions in the ratio of 1:2(M:L).



Scheme 1. synthesis path way of thiazolidine-4-carboxylic acid derivatives and its complexes.

FT- IR Spectra

Broad strong bands were displayed by IR spectra pertaining to ligands and metal complexes in the range of 3313-3510 cm^{-1} because of $\nu(\text{O-H})$ and a band at a range of 1635-1772 cm^{-1} could be attributed to stretching of C=O , while appearing of $\nu(\text{C=C})$ band occurred in the range of 1587-1622 cm^{-1} . Coordination of metal–ligand can be attributed to the difference in the position pertaining to the bands between the complexes and the ligands. The zwitterion like phenomenon in amino acids results in the appearance of the bands at 2694, 2574 and 2652 cm^{-1} in the spectrum pertaining to L^1 and L^2 . The phenomenon is a result of the formation pertaining to internal balance of salt of amino secondary (NH_2^+) and carboxylate group (COO^-) [19], as presented in Fig. 1. The coordination pertaining to metal ion with oxygen and nitrogen atoms is signified by the absence of these bands in metal complexes spectrum.

Uv-Visible spectra and magnetic susceptibility.

Four peaks were exhibited by the free ligands L^1 and L^2 in the electronic spectra that were assigned to $n - \sigma^*$, $n - \pi^*$ and $\pi - \pi^*$ transitions. A red shift and overlap of the peaks allowed distinguishing the spectrum of metal complexes, and a charge transfer peaks could be seen in the range of 300-500 nm as well as d-d transitions peaks in the visible region. At 670 and 660 nm, one low intense peak was exhibited by the spectrum of the Cu(II) complexes, which corresponded to transition from ${}^2\text{T}_2\text{g} \rightarrow {}^2\text{E}_\text{g}$ in the characteristic tetrahedral geometry[18]. Magnetic moment values of 1.34 as well as 1.37 B.M. were achieved with these complexes, which is in line with one unpaired electron. Single absorption band at 600 and 580 nm was displayed by the electronic spectra of the Fe(II) complexes, which

could be attributed to transition from ${}^5\text{T}_2\text{g} \rightarrow {}^5\text{E}_\text{g}$, as well as its exhibited magnetic moment values pertaining to 6.31 and 5.96 B.M. When high spin octahedral geometry is considered [20], these could also be normal values. At 570 and 620 nm, two peaks were exhibited in the visible region of VO(II) complexes for $\text{VO(L}^1\text{)}_2$, while at 570 and 730 nm for $\text{VO(L}^2\text{)}_2$, which could also be due to transitions ${}^2\text{B}_2 \rightarrow {}^2\text{B}_1$ and ${}^2\text{B}_2 \rightarrow {}^2\text{E}$, respectively. As per these assignments, VO(II) complexes are associated with square pyramid structure[21], and the magnetic moment values were 1.59 and 1.68 B.M for complexes, which denote one unpaired electron in d-orbital.

Microanalysis and metal:ligand ratio of complexes

The Job's method [22] was employed to determine the metal:ligand ratio pertaining to the complexes at a fixed pH and with maximum absorption wavelengths. Table 1 presents a summary pertaining to the results. It was found that the ligands formed 1:2 chelates along with Cu(II) , VO(II) and Fe(II) metal ions. The results concur with the values pertaining to the metal ions ratio, as obtained via flame atomic absorption shown in Table 1.

Mass spectra

The molecular ion peaks were seen with the mass spectra of ligands at $m/z=275$ with 20% abundance for L^2 and $m/z = 225$ with 60% abundance for L^1 , which correspond to $[\text{C}_{14}\text{H}_{13}\text{NO}_3\text{S}]^+$ and $[\text{C}_{10}\text{H}_{11}\text{NO}_3\text{S}]^+$ species, respectively. At $m/z = 132$ and 115, base peaks could be seen. The molecular ion peaks were exhibited by the mass spectra of $[\text{Cu(L}^1\text{)}_2] \cdot \text{H}_2\text{O}$, $[\text{Cu(L}^2\text{)}_2] \cdot 1/2\text{H}_2\text{O}$, $[\text{Fe(L}^1\text{)}_2(\text{H}_2\text{O})_2]$, $[\text{Fe(L}^2\text{)}_2(\text{H}_2\text{O})_2]$ and $[\text{VO(L}^1\text{)}_2] \cdot 2\text{H}_2\text{O}$ complexes at m/z

$z=529, 620, 538, 640$ and 549 , respectively, with low abundance, which were found to agree with the put forward formulas $[C_{20}H_{22}CuN_2O_7S_2]^+$, $[C_{28}H_{25}CuN_2O_{6.5}S_2]^+$, $[C_{20}H_{24}FeN_2O_8S_2]^{++}$, $[C_{28}H_{28}FeN_2O_8S_2]^+$ and $[C_{20}H_{22}N_2O_9S_2V]^{++}$.

1H NMR spectra of ligands

(2*R*,4*R*)- and (2*S*,4*R*)-diastereomer mixture is formed as the 2-Substituted thiazolidine-4-carboxylic acids possess a chiral carbon atom [23], as shown in Fig. 2. 1H NMR spectra of ligands L^1 and L^2 , Fig. 3 shown A multiplet signal in the range of 7.34-7.06 and 7.90-7.05 ppm, respectively, which were allotted to aromatic protons. A multiplet signal was seen as the protons were not equivalent. When compared to

protons on other ring carbon atoms, proton H2 are considered to be markedly deshielding, which could be because of the phenyl ring present on the same carbon atom. It was found that proton H4 resonated between 3.44 ppm and 3.83 ppm pertaining to L^2 and L^1 , respectively, based on the molecule's overall structure. At low field, a triplet was formed by the H4 proton of L^1 and L^2 , and overlapping doublets of doublets are caused by H5 protons, while the resonance of the proton H2 yielded a singlet at 5.6 and 6.7 ppm. At 9.19 ppm for L^2 and 9.8 ppm for L^1 , the proton appeared from the phenol group. However, the zwitter ion phenomenon led to disappearance of protons of carboxylic and amine groups [19].

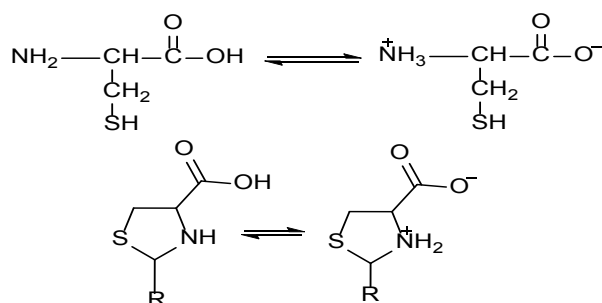


Fig. 1. the phenomenon of zwitter ion in amino acid and thiazolidine.

TABLE 1. Data of molar ratio and flame atomic absorption of metal complexes.

Complexes	Molecular weight	$(\lambda_{max}) nm$	Flame atomic absorption		M : L
			Calculated	Found	
$[Cu(L^1)_2].H_2O$	530.05	320	11.98	11.90	1:2
$[Cu(L^2)_2].1/2H_2O$	621.17	230	10.22	10.63	1:2
$[Fe(L^1)_2(H_2O)_2]$	540.35	320	10.36	11.36	1:2
$[Fe(L^2)_2(H_2O)_2]$	640.05	430	8.75	7.88	1:2
$[VO(L^1)_2].2H_2O$	551.45	310	9.24	9.33	1:2
$[VO(L^2)_2].2H_2O$	651.55	300	7.82	7.88	1:2

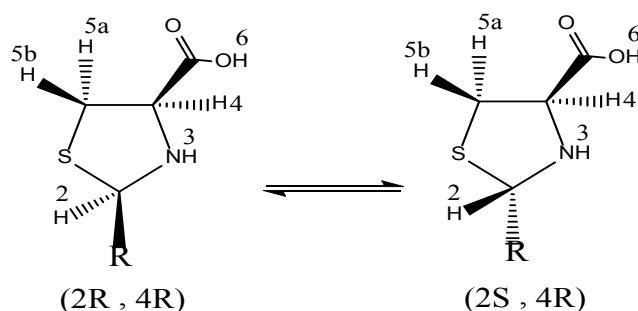


Fig.2. show isomers of 2-Substituted thiazolidine-4-carboxylic acids.

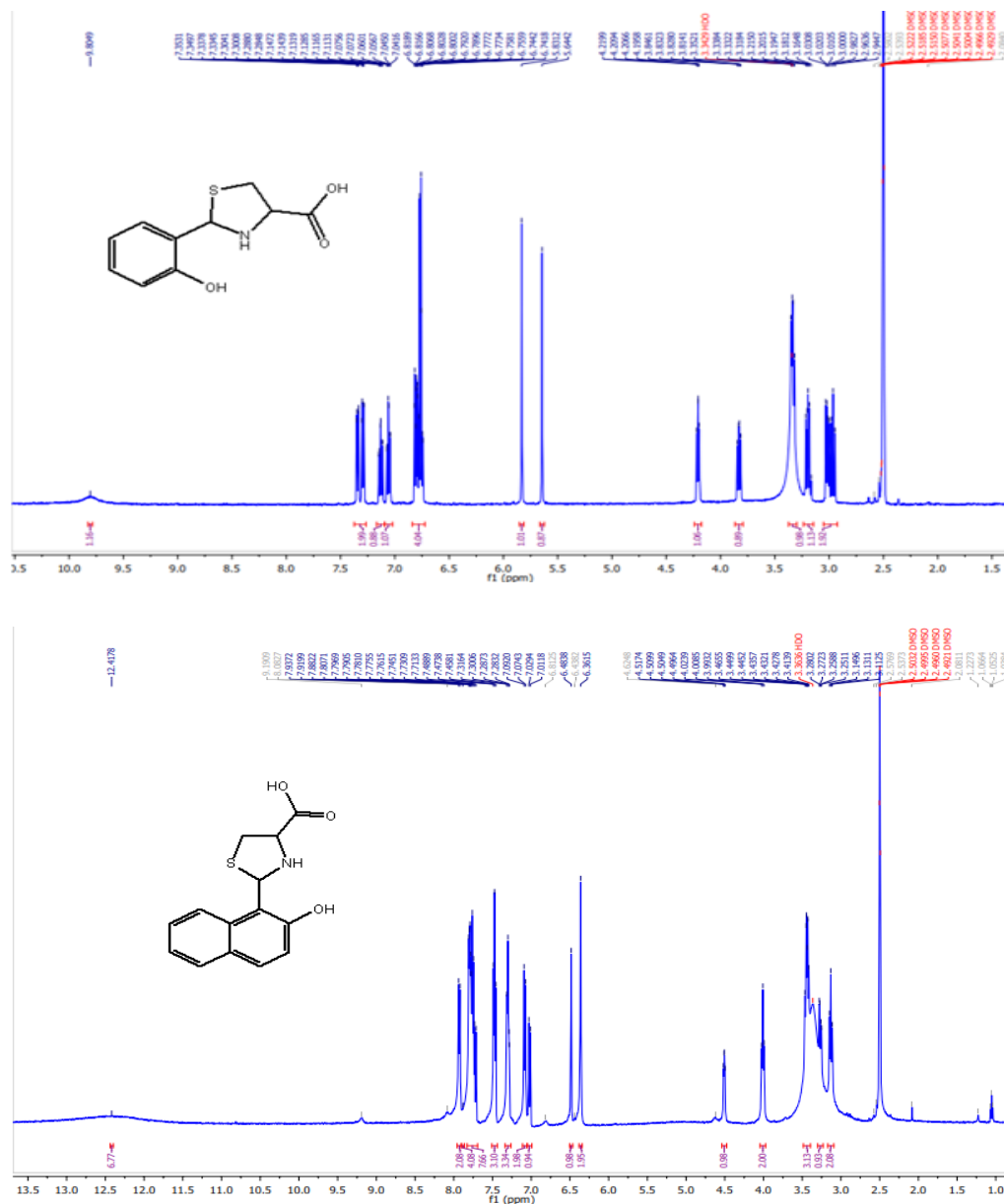


Fig. 3. ¹H NMR spectra of ligands.

Thermogravimetric analysis and molar conductivity

By maintaining a heating rate of 10°C/min, the complexes were subjected to thermal analysis to understand their thermal behaviour, while thermograms signify the presence of lattice as well as coordinated water pertaining to complexes molecules. In Fig.4 observe the complexes exhibited that they were thermally stable, with overall loss greater than 17% for copper complexes, 33% for iron complexes and 37% for oxovanadium complexes at temperatures of 700°C for all phases of thermal decomposition.

A three-stage decomposition pattern was observed with the thermograms of Cu(II) complexes; the first stage involved loss of lattice water molecules at 70 -120°C, and the next stages involved loss of C₅H₁₀ molecule at 200 -315°C and CO₂ molecule at 210 -325°C for CuL² and CuL¹, respectively. The third phase of the decomposition pattern of CuL¹ demonstrated losses of C₃H₅ at 325-680°C, whereas the CuL² decomposition pattern demonstrated losses of 2NH₂ at 307-680°C.

Five stages, two steps were observed based on the TG analysis of Fe(II) complexes, which

signify the removal of coordinated waters at a temperature range of 70 -200°C. The remaining phases of the thermal decomposition are depicted in Table 2.

A four and three-stages a decomposition pattern were observed with the thermograms of $[\text{VO}(\text{L}^1)_2]$ and $[\text{VO}(\text{L}^1)_2]$ complexes; The first stage refers to lose lattice water at 70-190°C and remaining phases are shown in the Table 2.

DMF solvent was employed to determine the molar conductivity of metal complexes, wherein values were found to lie in the range of 6-36 $\text{Ohm}^{-1} \text{cm}^2 \text{mol}^{-1}$, which support its non-electrolytic characteristic [24]. Therefore, formulation of the complexes could be done as $[\text{M}(\text{L})_2] \cdot \text{XH}_2\text{O}$ [where X=numbers of water molecules; M= Cu(II), Fe(II)(H₂O) and VO(II); L= L¹ and L²].

Antibacterial assay

Based on their *in vitro* antibacterial activities, screening of the synthesized compounds is done by measuring the inhibition zone in

terms of millimetre via the paper disc-agar diffusion technique. As a control, the antibiotic Ciprofloxacin was employed against negative bacteria (*Pseudomonas aeruginosa*), while Amoxicillin was employed against positive bacteria (*Streptococcus epidermis*). The observations of the antibacterial activity are depicted in Table 3. All compounds were seen to show activity against both bacterial species, when antibacterial activity pertaining to free ligands as well as its metal complexes was compared. Thus, less effectiveness was found with Cu(II) and VO(II) complexes, which could be because of coordination amongst certain biological active sites pertaining to the ligands molecules (N/O atoms) along with the metals ion. Fe(II) complexes demonstrated the highest activity[25,26] against two kinds of bacteria in comparison with drug standard and ligands molecules. The higher antimicrobial activity of metal complexes could be because of the impact of the chelation theory [27], which enabled improved intracellular penetrability of the complexes.

TABLE 2. TG analysis data of metal complexes.

Complexes	Stages	Temp. range °C	Decomposition parts	Weight lose %	
				Calculated	Found
$[\text{Cu}(\text{L}^1)_2] \cdot \text{H}_2\text{O}$	1	88-210	1H ₂ O	3.39	3.41
	2	210-325	CO ₂	8.59	6.94
	3	325-680	C ₃ H ₅	8.76	8.6
$[\text{Cu}(\text{L}^2)_2] \cdot 1/2\text{H}_2\text{O}$	1	50-200	1/2H ₂ O	1.44	1.18
	2	210-325	C ₅ H ₁₀	11.43	12.47
	3	307-680	2NH	5.53	5.85
$[\text{Fe}(\text{L}^1)_2(\text{H}_2\text{O})_2]$	1	20-175	2H ₂ O	6.66	6.18
	2	175-280	CO ₂	8.73	8.49
	3	280-400	NH	3.26	2.42
	4	400-620	C ₂ H ₅	6.51	7.09
$[\text{Fe}(\text{L}^2)_2(\text{H}_2\text{O})_2]$	1	100-225	2H ₂ O	5.62	6.01
	2	225-425	NH ₂	2.64	3.09
	3	225-550	CS	7.48	8.55
	4				
$[\text{VO}(\text{L}^1)_2] \cdot 2\text{H}_2\text{O}$	1	885-200	2H ₂ O	6.53	5.60
	2	200-345	C ₆ H ₆ O	18.25	17.15
	3	345-550	CS	10.45	9.19
	4	550-675	CH ₂ N	7.42	7.23
$[\text{VO}(\text{L}^2)_2] \cdot 2\text{H}_2\text{O}$	1	70-225	2H ₂ O	5.52	5.27
	2	225-380	C ₄ H ₅ N	10.08	10.14
	3	380-675	VO	12.04	11.02

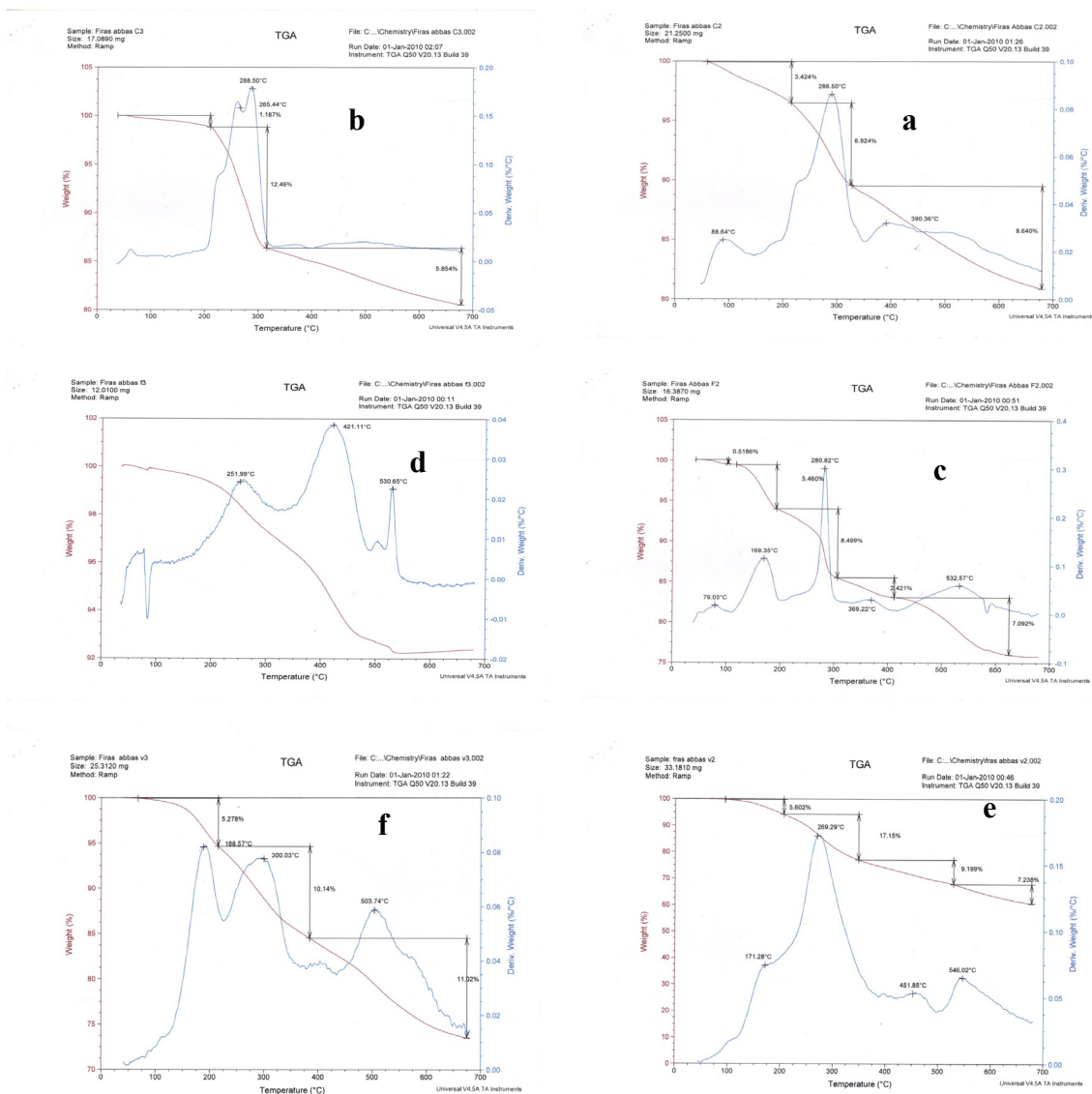


Fig. 4. TGA curves of a: $[\text{Cu}(\text{L}^1)_2] \cdot \text{H}_2\text{O}$, b: $[\text{Cu}(\text{L}^2)_2] \cdot 2\text{H}_2\text{O}$, c: $[\text{Fe}(\text{L}^1)_2(\text{H}_2\text{O})_2]$, d: $[\text{Fe}(\text{L}^2)_2(\text{H}_2\text{O})_2]$, e: $[\text{VO}(\text{L}^1)_2] \cdot 2\text{H}_2\text{O}$, f: $[\text{VO}(\text{L}^2)_2] \cdot 4\text{H}_2\text{O}$ complexes.

TABLE 3. Antibacterial activity data of studied compounds.

Compounds	Diameter of inhibition zone in mm	
	<i>Streptococcus epidermis</i>	<i>Pseudomonas aeruginosa</i>
L ¹	18	16
L ²	20	22
$[\text{Cu}(\text{L}^1)_2]$	16	15
$[\text{Cu}(\text{L}^2)_2]$	19	18
$[\text{Fe}(\text{L}^1)_2(\text{H}_2\text{O})_2]$	25	30
$[\text{Fe}(\text{L}^2)_2(\text{H}_2\text{O})_2]$	23	25
$[\text{VO}(\text{L}^1)_2]$	10	14
$[\text{VO}(\text{L}^2)_2]$	8	22
Amoxicillin	22	----
Ciprofloxacin	----	17

Computational study

The geometry optimisation of ligands and their complexes was conducted by the density function theory. Figures 5 and 6, respectively, depict the optimised structures of the ligands and complexes with atom labelling. The bond angles, bond lengths, and dihedral angles are shown in Table 4. Deprotonation of the ligand molecules occur, making them behave as a bidentate monoanionic ligands framework that possesses an N, O⁻ binding mode. The bond lengths that were calculated for C1-N and C6-O8 in ligands were found to lie in the range of 1.37-1.84 Å, which can be deemed as approximate value pertaining to a single bonds length. In the complexes molecules, these bonds were found to get elongated by 0.02-0.08 Å due to the coordination occurring between lone pair on the N and O atoms as well as d-orbital pertaining to metals atoms. There was no significant difference found amongst other bonds

length and triangles pertaining to complexes molecules and ligands. However, a change of 3.8-6.4 degree was seen in C1-C6-O8 angle due to the interaction of O8 atom with that of the metal ions. The dihedral angles pertaining to ligands were calculated and found to be (C2-S-C4-C14= 89.4° and 88.2°) and (C4-N-C1-C6= 83.4° and 84.7°), which signify that the ligand molecules possess a rotational structure. This case is inverse when it comes to metal complexes molecules that possess approximate planer structure pertaining to the same position (C2-S-C4-C14= 137.1°- 168.5°) and (C4-N-C1-C6= 142.8°- 170.8°), as presented in Table 4. A certain deviation could be seen from the octahedral, tetrahedral as well as square pyramidal geometry pertaining to the values of theoretical bonds angle (M-N and M-O) as well as triangle (N-M-O) with regards to the Fe(II), Cu(II) and VO(II) complexes[24].

TABLE 4. Some of the structural properties of the studied molecules.

Molecules	Bonds length (Å)							
	C4-N	C1-N	C4-S	C2-S	C1-C2	C6-O8	M-O	M-N
L ¹	1.48	1.43	1.76	1.76	1.56	1.37	----	----
L ²	1.49	1.40	1.84	1.84	1.51	1.37	----	----
[Cu(L ¹) ₂]	1.49	1.48	1.73	1.77	1.55	1.45	1.84	1.85
[Cu(L ²) ₂]	1.51	1.41	1.83	1.82	1.53	1.44	1.85	1.82
[Fe(L ¹) ₂ (H ₂ O) ₂]	1.44	1.47	1.76	1.75	1.57	1.43	1.88	1.87
[Fe(L ²) ₂ (H ₂ O) ₂]	1.46	1.45	1.81	1.80	1.52	1.42	1.87	1.86
[VO(L ¹) ₂]	1.43	1.49	1.77	1.77	1.56	1.43	1.87	1.89
[VO(L ²) ₂]	1.45	1.46	1.86	1.85	1.54	1.43	1.87	1.86

Molecules	Bond angles (°)				Dihedral angles(°)			
	C1-N-C4	N-C1-C2	C1-C6-O8	N-M-O	C1-N-C4-C14	C4-N-C1-C6	C2-S-C4-C14	C2-S-C4-C14
L ¹	112.2	108.6	113.3	----	141.7	83.4	122.0	89.4
L ²	112.7	108.5	113.4	----	136.7	84.7	113.9	88.2
[Cu(L ¹) ₂]	108.5	108.3	117.1	114.7	187.9	166.2	126.4	168.5
[Cu(L ²) ₂]	106.9	103.9	119.7	91.3	170.8	170.8	177.1	145.2
[Fe(L ¹) ₂ (H ₂ O) ₂]	107.4	106.4	117.8	93.1	174.9	143.7	86.5	137.1
[Fe(L ²) ₂ (H ₂ O) ₂]	106.3	99.7	116.3	86.0	172.2	142.8	174.7	141.5
[VO(L ¹) ₂]	103.1	102.0	118.2	87.3	172.3	144.2	176.1	143.7
[VO(L ²) ₂]	111.4	109.1	118.7	95.7	166.5	163.1	168.2	162.2

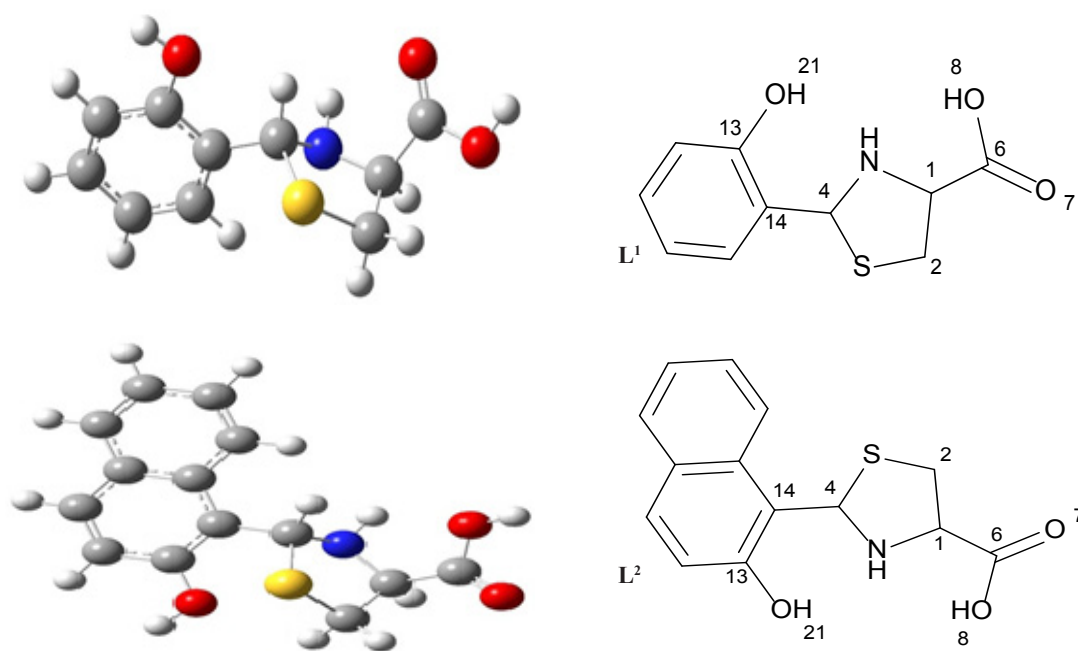


Fig. 5. Optimization geometries structures of the Ligands with its labeling.

The ligand molecules' atomic charges as computed using the Mulliken technique[28] are depicted in Table 5. As observed, oxygen and nitrogen atoms were found to possess high charge electrophilic density. The O8 atom had charge of -0.565 and -0.577, while O21 atom possessed charge of -0.393 and -0.347. Hence, it can be said that a higher ability for coordination of the metal ion was associated with the O8 atom versus O21 due to its higher basicity[29].

Table 6 provides a summary of the binding energy, total energy, HOMO-LUMO energy gap, heat of formation and dipole moment that were computed by employing the same method with basis set. The chemical activity of the molecule is shown by the values of dipole moment and

energy gap ($\Delta E_{\text{LUMO-HOMO}}$) [30]. Based on the values listed in Table 6, higher reactivity was associated with the L^2 molecule versus L^1 molecule ($\Delta E_{\text{LUMO-HOMO}}$ of $L^1 = 0.1477$ Ha., $L^2 = 0.1197$ Ha. and μ of $L^2 = 6.538$ Debye $L^1 = 6.401$ Debye), while lower reactivity was associated with the complexes molecules versus ligand molecules, with the exception of $[\text{Fe}(L^2)_2(\text{H}_2\text{O})_2]$, $[\text{VO}(L^1)_2]$ and $[\text{VO}(L^2)_2]$ molecules. This could be because of the presence of iron and oxovanadium atoms, or stereo configuration associated with these complexes. These outcomes are good and according to the results attained from biological activity tests [31]. The high stability pertaining to complexes molecules was signified with the heat of formation as well as binding energies values versus ligands molecules [32].

TABLE 5. The Mulliken atomic charges of ligand molecules.

Molecules	N	C1	C2	C4	C6	S	O7	O8	C13	C14	O21
L^1	-0.496	-0.055	-0.306	-0.413	0.493	-0.277	-0.522	-0.565	0.213	0.194	-0.393
L^2	-0.448	-0.173	-0.343	-0.431	0.538	-0.283	-0.543	-0.577	0.384	0.245	-0.347

Conclusion

The structural information acquired from synthesized compounds is in line with the data stated in this paper. The presence of the ligands molecules in the form of zwitterions was confirmed via the IR and NMR spectra, and this form was found to disappear post coordination with metals. Based on the study pertaining to the complexes' correlation ratio and the atomic absorption analysis, it can be said that the ligands tend to act as bidentate and mono-ionic, and their interaction pertaining to metals was in the mole ratio of 1:2(M:L). The electronic spectra as well as magnetic susceptibility provided information regarding the complexes' geometry, which were found to be octahedral, tetrahedral and square pyramidal pertaining to Fe(II), Cu(II) and VO(II) complexes, respectively. As per TG analysis and conductivity, all complexes were found to possess lattice water and non-electrolyte, and iron complexes possessed two coordinated water molecules.

The compounds' antimicrobial screening indicated that the iron complexes demonstrated high activity in comparison with parent ligands, while Cu(II) and VO(II) complexes were not quite effective. These results were found to be in line with the theoretical DFT calculation, including $\Delta E_{\text{LUMO-HOMO}}$ as well as dipole moment. The DFT calculation also specifies that the complex molecules possess geometry deviation pertaining to the structures, which were very stable and were found to interact with ligands molecules via N and O atoms.

Acknowledgement

The researchers express their gratitude to the Department of Chemistry, Faculty of Education of Pure Sciences, Basrah University in Iraq, for supporting facilities that include laboratories and infrared measurements.

References

- Oya M., Baba T., Kato E., Kawashima Y. and Watanabe T. Synthesis and antihypertensive activity of N-(mercaptoacyl)-thiazolidinecarboxylic acids. *Chem. Pharm. Bull.*, **30**, 440-461(1982).
- Restelli A., Annunziata R., Pellacini F. and Ferrario F. NMR Determination of absolute configurations in 2-alkylthiazolidine-4-carboxylic acids. *J. Heterocycl. Chem.*, **27**, 1035-1039(1990).
- Patek M., Drake B. and Lebl M. Solid-phase synthesis of 'small' organic molecules based on thiazolidine scaffold. *Tetrahedron Lett.*, **36**, 2227 - 2230(1995).
- Refouvelet B., Pellegrini N., Robert J.-F., Crini G., Blacque O. and Kubicki M. M. Synthesis and stereochemical studies of 2-substituted thiazolidine-4-carboxamide derivatives. *J. Heterocycl. Chem.*, **37**, 1425 -1430(2000).
- Weber H.U., Fleming J.F. and Miquel J. Thiazolidine-4-carboxylic acid, a physiologic sulfhydryl antioxidant with potential value in geriatric medicine. *Arch. Gerontol. Geriatr.*, **1**, 299-310(1982).
- Ferandez X., Fellous R., Lizzani-Cuvelierx L., Loiseaux M. and Dunach E. Chemo- and regioselective synthesis of alkyl-3-thiazoline carboxylates. *Tetrahedron Lett.*, **42**, 1519 -1521(2001).
- Novo O., Balcells M., Canela-Garayoab R. and Eras J. Combining a flow reactor with spray dryer to allow the preparation of food-grade quality sodium 2- polyhydroxyalkyl-1,3-thiazolidine-4-carboxylates with a low environmental impact. *RSC Adv.*, **6**, 6651-6657(2016).
- Nair M. S. and Neelakantan M.A. Solution behaviour of mixed ligand complexes of nickel(II) involving penicillin group dru and sulfur containing ligands under physiological conditions. *J.Ind. Chem.Soc.*, **77**(8), 373-375(2000).
- Lucke A.J., Tyndall J.D.A., Singh Y. and Fairlie D.P. Designing supramolecular structures from models of cyclic peptide scaffolds with heterocyclic constraints. *J. Mol. Graphics & Modell.*, **21**(5), 341-355(2003).
- Abed-Rahman El-Gazzar B.A., Gaafar A.M. and Aly S.A. Design, synthesis, and preliminary evaluation as antimicrobial activity of novel spiro-1, 3-thiazolidine C- acyclic nucleoside analogs. *J.Sulfur. Chem.*, **29**(5), 549-558(2008).
- McOmie J. F. W., "Protective groups in organic chemistry" [Russian translation], Moscow, 191 (1976).
- Negrete G. R., Mahindaratne M. P. D., Mfuh A. M. and Quintero M. V., US Patent 2011 0 268 653(2011).
- Hossain M. S., Zakaria C. M. and Kudrat-E-Zahan M. Metal Complexes as Potential Antimicrobial Agent: A Review. *Am. J. Heterocyclic Chem.*, **4**(1), 1-21(2018).

14. Ghazi D., Rasheed Z. and Yousif E. A Review of Organotin Compounds: Chemistry and Applications. *Arch. Org. Inorg. Chem. Sci.*, **3**(3), 344-352(2018).
15. Balouiri M., Sadiki M. and Koraichi Ibsouda S. Methods for *in vitro* evaluating antimicrobial activity: A review. *J. Pharm. Anal.*, **6**(2): 71-79(2016).
16. Belkafouf N., Baara F.T., Altomare A., Rizzi R., Chouaih A., Djafri A. and Hamzaoui F. Synthesis, PXRD structural determination, Hirshfeld surface analysis and DFT/TDDFT investigation of 3N-ethyl-2N'-(2-ethylphenylimino) thiazolidin-4-one. *J. Mol. Str.*, **1189**, 8-20 (2019).
17. Yang Y., Weaver M.N. and Merz K.M. Assessment of the "6-31+G** + LANL2DZ" Mixed Basis Set Coupled with Density Functional Theory Methods and the Effective Core Potential: Prediction of Heats of Formation and Ionization Potentials for First-Row-Transition-Metal Complexes. *J. Phys. Chem. A*, **113**, 9843-9851(2009).
18. Wahba O.A.G., Hassan A.M., Naser A. M. and Hanafi A.M. Preparation and Spectroscopic Studies of Some Copper and Nickel Schiff Base Complexes and their Applications as Colouring Pigments in Protective Paints Industry. *Egypt. J. Chem.* **60**(1), 25- 40 (2017).
19. Howard-Locck H.E., Lock J.L., Martinsp M.L., Smalley S. and Bell R.A. Amino-acid zwitterion equilibria: vibrational and nuclear magnetic resonance studies of methyl-substituted thiazolidine-4-carboxylic acids. *Can. J. Chem.*, **64**, 1215-1219(1986).
20. Ali, A.M. Synthesis and Characterization of the Ligand 2-[(6-Nitro-2-benzothiazolyl)azo]-4,6-dimethylphenol (6-NBTADMP) and It's Complexes with Fe(II), Co(III), Ni(II), Cu(II), Zn(II), Cd(II),Pd(II) and Ag(I) Ions. *National Journal of Chemistry*, **28**,676- 686(2007).
21. Pethe G.B., Yaul A.R. and Aswar A.S. Synthesis, characterization, electrical and catalytic studies of some coordination compounds derived from unsymmetrical Schiff base ligand. *Bull. Chem. Soc. Ethiop.*, **29**(3), 387-397(2015).
22. Mabrouk M., Hammad S. F., Abdelaziz M. A. and Mansour F. R. Ligand exchange method for determination of mole ratios of relatively weak metal complexes: a comparative study. *Chem. Cen. J.*, **12**(1), 1-7(2018).
23. Ershov A.Y., Nasledov D.G., Lagoda I.V. and Shamanin V.V. Synthesis of 2-substituted (2R,4R)-3-(3-mercaptopropionyl) thiazolidine-4-carboxylic acid. *Chem.Hetrocyclic Comp.*, **50**(7), 1032-1038 (2014).
24. Chand S., Tyagi M., Tyagi P., Chandra S. and Sharma D. Synthesis, characterization, DFT of novel, symmetrical, N/O-donor tetradentate Schiff's base, its Co(II), Ni(II), Cu(II), Zn(II) complexes and their in-vitro human pathogenic antibacterial activity. *Egypt. J. Chem.* **62**(2), 291-310(2019).
25. Mishra L., Said M.K., Itokawa H. and Takeya K. Antitumor and Antimicrobial Activities of Fe(II)/Fe(III) Complexes Derived from some Heterocyclic Compounds. *Bioorg. Medici. Chem.*, **3**(9), 1241-1245(1995).
26. Pansuriya P.B., Dhandhukia P., Thakkar V and Patel M.N. Synthesis, spectroscopic and biological aspects of iron(II) complexes. *J. Enz. Inhib. Medici. Chem.*, **22**(4), 477-487(2007).
27. Sengupta S. K., Pandey O.P., Srivastava B. K. and Sharma V. K. Synthesis, structural and biochemical aspects of titanocene and zirconocene chelates of acetylferrocenyl thiosemicarbazones. *Transition Metal Chemistry*, **23**(4), 349-353(1998).
28. Ogorodnikova N. A. On invariance of the Mulliken substituent-induced charge changes in quantum-chemical calculations of different levels of different levels. *J.Mol.Struct.*, **894**, 41-49(2009).
29. Akbari A. and Alinia Z. Synthesis, characterization, and DFT calculation of a Pd(II) Schiff base complex. *Turk.J.Chem.*, **37**, 867-878(2013).
30. Zhou Z. and Parr R.G. Activation hardness: new index for describing the orientation of electrophilic aromatic substitution. *J.Am.Chem.Soc.*, **112**, 5720-5724(1990).
31. Al-Masoudi W.A., Othman R.M., Al-Asadi R.H. and Ali M.A. Antimicrobial activity and computational study of new cobalt(II) complex of benzothiazole derivative. *Bas.J.Vet.Res.*, **15**(4), 214-229(2016).
32. Esmaielzadeh S. and Mashhadiagha G. Formation constants and thermodynamic parameters of bivalent Co, Ni, Cu and Zn complexes with Schiff base ligand: Experimental and DFT calculations. *Bull. Chem. Soc. Ethiop.*, **31**(1), 159-170(2017).

تحضير ودراسة فعالية ضد البكتيرية وحسابات نظرية دالة الكثافة لبعض مشتقات ثايزولدين- ٤-حامض الكاربوكسيل ومعداتها مع النحاس الثنائي والحديد الثنائي والاكسوفنيديوم الثنائي

فiras عباس نوار^١، رافد حميدان الاسدي^٢ و داود سالم عبد^٢

^١ مديريّة التربية في ذي قار - وزارة التربية - ذي قار - العراق.

^٢ قسم الكيمياء - كلية التربية للعلوم الصرفة - جامعة البصرة - العراق

ان تفاعل الحامض الاميني (L- Cysteine) مع ٢-هيدروكسي نفتلديهايد و ٢-هيدروكسي بنزلديهايد اعطى الليكندين L¹ و L² على التوالي ، شخّصت الليكندات من خلال البيانات الفيزيائية والطيفية . ايضا تضمنت الدراسة تحضير متراكبات تناسقية جديدة من تفاعل الليكندين L¹ و L² مع ايونات النحاس الثنائي والحديد الثنائي والاكسوفنيديوم الثنائي بنسبة ارتباط (٢:١) فلز : ليكند ، وباعتماد على اطيف تحت الحمراء والاطيف الالكترونية واطيف الكتلة والامتصاص الذري اللهيبي والحساسية المغناطيسية والتحليل الحراري الوزني تم استنتاج الشكل المقترح للمتراكبات المحضرة. تم تقييم فعالية ضد البكتريا للمركبات المحضرة ضد نوعين من البكتريا وهي *Pseudomonas aeruginosa* و *Streptococcus epidermis* حيث اظهرت الدراسة ان جميع المركبات لها فعالية متفاوتة ضد هذه البكتريا . علاوة على ذلك فقد تم دراسة التركيب الجزيئي وحساب الطاقات للمركبات المحضرة باستخدام نظرية دالة الكثافة (DFT) عند المستوى B3LYP ومن خلال النتائج لوحظ ان هناك تطابق بين الحسابات النظرية والنتائج العملية .